PRATHAM

IIT BOMBAY STUDENT SATELLITE

Preliminary Design Report

Thermals Subsytem

By

Ayanangshu Dey

Haripriya

Manas Rachh

Nithin Mannil

Sachin A S

Sujay Desai

Department of Aerospace Engineering,

Indian Institute of Technology, Bombay

April, 2009

Acknowledgement

I would like to thank Prof Kannan Iyer, Prof Mahulikar and Dr Krishnendu Sinha for their valuable inputs. I would also like to thank the entire satellite team for their support.

Contents

List of figures

1. Introduction

The environment upto a height of around 500km above the Earth is strongly affected by the presence of the denser layers of the atmosphere and by interaction with the hydrosphere, and thus experience relatively mild conditions of temperature. However, above 500km, the atmosphere becomes too thin to moderate the ambient thermal conditions and consequently, the environment above such a height is prone to extremes of temperature, being directly exposed to solar radiation and deep space.

Spacecraft, which are primarily intended to perform scientific missions which require them to be positioned far away from the Earth's surface, spend their entire lifetime in the harsh environments of the upper atmosphere or interplanetary space. Being electromechanical systems, however, these spacecraft also have certain requirements of temperature ranges outside which their systems cannot function viably. Hence, every such spacecraft must incorporate a thermal subsystem to achieve an optimal thermal environment for its smooth functioning, through either active or passive means.

The requirements of thermal control and the challenges involved in realizing these in case of nanosatellites in Low Earth Orbit (LEO) are unique. The IIT Bombay Student Satellite, PRATHAM, belongs to this class of satellites, having a mass of less than 10kg and orbiting in a LEO of approximate altitude 700km. The Thermals Subsystem of PRATHAM aims to maintain a cycle of temperature within the satellite which has a narrow range and lies around the normal terrestrial temperatures, minimize spatial gradients of temperature, dissipate excess heat generated by other subsystems and maintain sensitive components within their specified functional ranges of temperature.

2. Requirements & Constraint Analysis

This chapter is divided into two parts. In the first part we will discuss the requirements of other sub-systems which need to be addressed by the thermals subsystem. In the second part we shall discuss issues that would imposed constraints on the flight model but need not be considered in this design phase.

2.1 Requirements of other sub-system

2.1.1 Requirements from Power Sub-System to Thermals Sub-System

- Thermals Sub-System shall protect the solar panels from heating above 70^0C.
- The optimal operating range of the battery is from 5^0 to 20^0 C. The acceptable operating range is 0^0 to 30^0 C. The thermals sub system shall try and maintain the battery within its optimal operating range. If that is not possible the battery must be maintained in the acceptable operating range.
- They shall remove the excessive heat from Power Circuits, since the temperature range of the components (industrial grade) is -40^0 to $+85^0$ C.

2.1.2 Requirements from Communication and Ground Station Sub-System to Thermals Sub-System

- Thermals Sub-System shall protect the monopoles from heating above 100^0C.
- They shall remove the excessive heat from the 2 Monopole circuits, since the temperature range of the components (industrial grade) is -40^0 to $+85^0$ C.

2.1.3 Requirements from On Board Computer Sub-System to Thermals Sub-System

- They shall remove the excessive heat from OBC Circuits, since the temperature range of the components (industrial grade) is -40^0 to $+85^0$ C.

The aim of the thermal subsystem is to satisfy all these requirements. The most stringent requirement is maintaining the temperature of the battery. In the next chapter we will look into the design procedure and performing the thermal analysis of the satellite. This will help us in deciding the required coatings and paints in order to maintain the temperatures of the various components within specified limits.

2.2 Constraint Analysis

In this part we shall discuss issues that need not be addressed in this design stage but may be concerns in the later design stages. We will be using paints as coatings to obtain desired values of absorptivity and emissivity. With time the molecules of these paints tend to evaporate. This issue is called out gassing. The effect of out gassing on the change of surface properties has not been addressed in this phase. Characterization of material properties is another issue. The problem is that the properties of the materials are a function of temperature and medium. One would ideally want no dependence on temperature and medium. So it is necessary to characterize the thermal coatings and paints in vacuum and the expected thermal environment of the satellite. The methodologies and equipment required for such characterization are not yet known.

3. Thermal Control Design

In this chapter, we will first look into the determination of the temperature of the body of the satellite. Different aspects like the detumbling mode, the effect of applying coating, validation of the models and grid convergence shall be discussed in detail. The simulations have been carried out using MSC NASTRAN which is a standard code for solving thermal problems. Next, once the thermal analysis is performed and the model validated, we will look into the design philosophy for maintain the temperature of the satellite within suitable limits. Limitations of the current model and how a detailed analysis will be carried is also discussed in this chapter.

3.1 Thermal Analysis

Simulations have been carried out for 2 cases. In one case no coating is applied where as in the other one two of the faces are coated with OSR. Unless mentioned, any data presented is valid for both the models

3.1.1 Basic Nomenclature & Definitions

Side facing the Sun (for the maximum time) – SS

Side opposite to the sun facing side – ASS

Side facing the earth – Nadir

Side opposite to Nadir – Zenith

The side whose normal is aligned with the velocity vector – Leading

The side opposite leading – Lagging

Internal radiation refers to the radiation exchange between the internal faces of the satellite

3.1.2 Assumptions

The flux is calculated for the 1030 sun synchronous orbit (calculations shown in Appendix A). The assumptions in the calculation of flux are that the sun is at infinity. The satellite enters the shadow region sharply. The control law is working. The flux reflected from the surface of the earth is not considered. Only the satellite body has been modeled. The other components have not been included. Heat dissipation of the various circuits is not accounted for. Internal radiation

is absent. Detumbling mode of the satellite has not been analyzed in these two models. Initial constant temperature of 300 K is assumed. The coating if applied has zero thickness and do not have any thermal inertia. All the heat absorbed by the solar panel goes in heating up the satellite.

3.1.3 Geometry

We have analyzed the satellite as a cube of side 23.5cm. The thickness of the satellite is 3 mm. The material of the satellite body is Al T 6061. Four of the faces viz. SS, Leading, Lagging and Zenith have solar panels. The surface of the solar panel is a square of size 21.5 cm. The thickness of the solar panel is 6 mm. The material used for the solar panel substrate is Kapton. The solar panels are placed with a clearance of 1 cm on each side. In model 1, there are no coatings. Model 2 is coated with OSR on Nadir and ASS.

3.1.4 Material properties

Aluminium:

Conductivity (K_{al}) – 237 W / (m-K)

Density (ρ_{al}) – 2700 kg/m^3

Specific heat capacity (C_{al}) – 880 J / (kg-K)

Absorptivity (α_{al}) – 0.2

Emissivity (ε_{al}) – 0.031

Solar Panel Substrate:

Conductivity (K_{sp}) – 0.192 W / (m-K)

Density (ρ_{sp}) – 2700 kg/m^3

Specific heat capacity (C_{sp}) – 755 J / (kg-K)

Absorptivity (α_{al}) – 0.75

Emissivity (ε_{al}) – 0.85

OSR

Absorptivity (α_{al}) – 0.15

Emissivity (ε_{al}) – 0.85

3.1.5 Elements

The model has been meshed using a structured grid. Hex8 elements were used. The maximum size of any element is 6 cm. Total number of elements were 352.

3.1.6 Loads & Boundary Conditions

- Initial Temperature – 300 K
- Flux calculated for 1030 sun synchronous orbit
- Radiation Boundary condition

3.1.7 Results

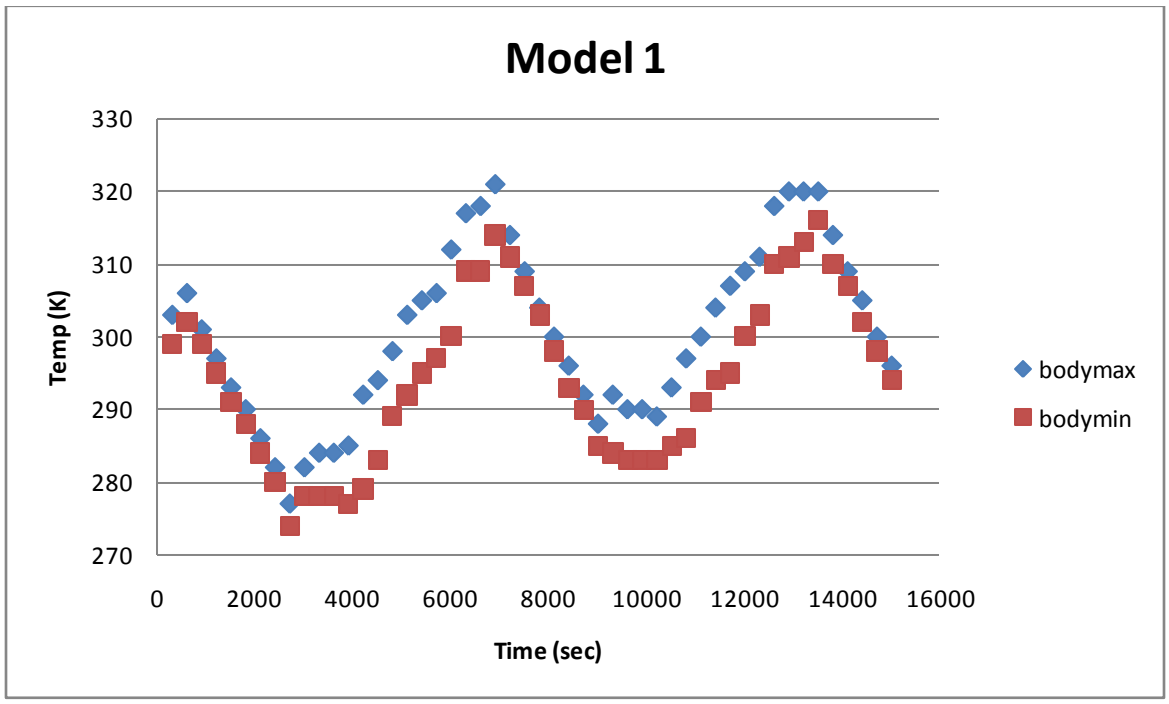

Figure 1: Satellite body temperature as a function of time (Model 1)

Figure 2: Satellite body temperature as a function of time (Model 2)

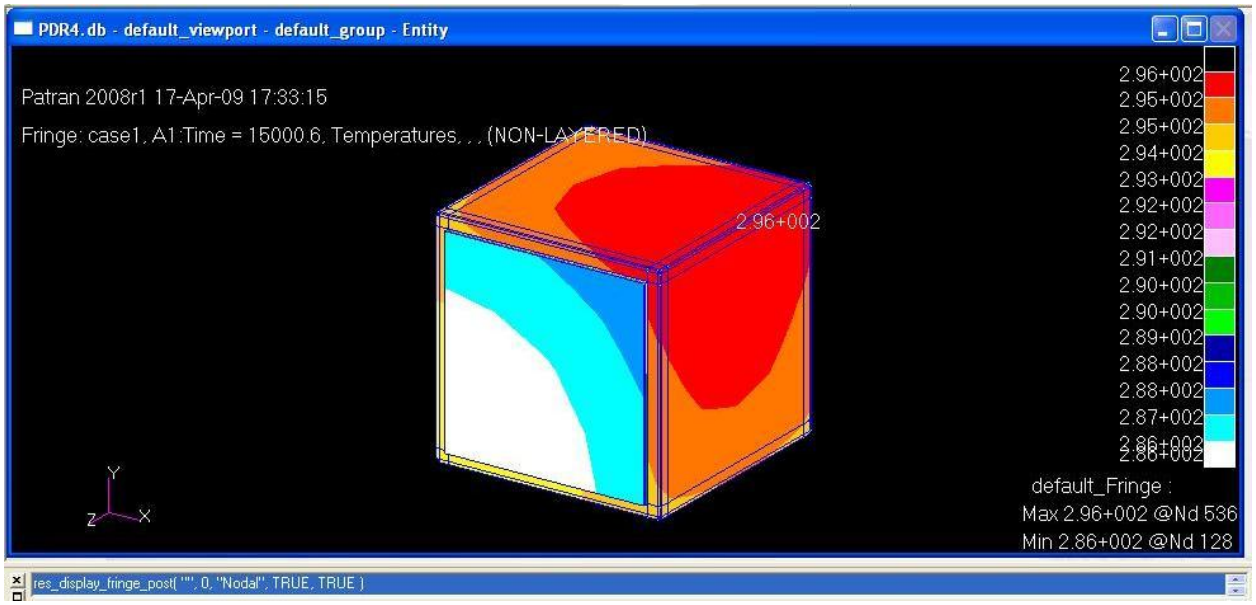

Figure 3: Temperature Contours for Model 1 at t=15000 sec

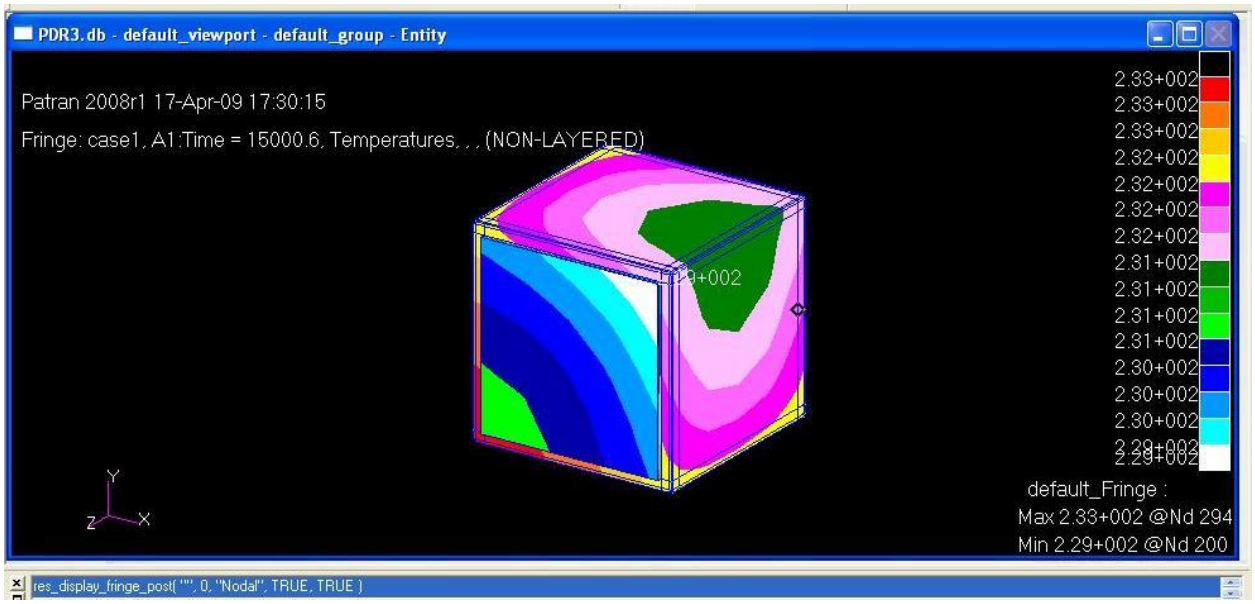

Figure 4: Temperature contours for Model 2 at t=15000 sec

Comments:

These graphs represent the maximum and minimum temperature of the body at every instant. The difference between the two graphs gives the spatial gradient at every time instant. The temporal range for model1 is 35 K whereas that for model2 is 30 K. The average temperature of model1 is around 302 K where as that for model2 is 245 K. Thus from this it is clear that applying OSR on both Nadir and ASS the average temperature drops considerably. But this picture is not an exact representative of reality since there are a lot of assumptions involved. Also it is observed that it takes around 2 cycles for the temperature to stabilize. This may not hold true once detumbling is also considered. Also it is to be noted that the overall maximum and minimum temperatures are observed at the solar panels. In model1 the maximum and minimum solar panel temperatures are 330 K and 284 K respectively where as in model2 they are 284 K and 229 K respectively. This is because of the very low conductivity of the solar panels.

3.1.8 Addressing the assumptions

Initial temperature of 300 K: The final solution is independent of the initial temperature boundary condition. It has been shown by simulations as well. The only thing that may change is the time required for the thermal cycle to stabilize

Only the body of the satellite has been modeled: This is a design philosophy. It becomes too complicated to model the complete satellite. Hence we will be modeling the satellite in parts and appropriately change the boundary conditions as required. This shall be discussed further in detail in the Section 3.2.

Internal radiation not included: Various attempts were made to incorporate internal radiation into the model. NASTRAN has a function for radiation enclosures which is used for its modeling. The working of that module of NASTRAN is not very clear and the solutions appeared to be incorrect. Just by adding enclosure radiation the temperatures went up by 100 K. Another model which was suggested to us by Prof Barve from ISAC was to assume that the sides are radiating to a fixed temperature of 293 K. In this case the solution did not converge even for small time steps. The results gave in negative temperatures which is not physical. A methodology needs to be thought for solving this problem as soon as possible.

Heat dissipation not included: This will be included in the later models. Once the issue of radiation enclosures is resolved, we will incorporate the heat dissipation terms.

All the heat absorbed by the solar panel goes in heating up the satellite: This was assumed because up to a long time the efficiency of the solar panels was not fixed. This will be incorporated in the future models.

Detumbling: Simulations are yet to be carried out to study the effect of detumbling of satellite.

3.1.9 Validation

Two of the modules of NASTRAN were used to carry out the simulations namely conduction and radiation. Each of these has been validated by test problems whose solution is known.

Conduction

For the conduction model, we considered a plate which had all sides fixed temperature boundary condition and evaluated the steady state temperature contours. Three of the sides were maintained at 0 ^{0}C and the fourth side at 200 ^{0}C. A good way to check the working of this model is that the results should be independent of the value of conductivity. The error in the overall

results can be found out by comparing the temperature from simulations with that calculated by theory at the centre of the plate. From theoretical calculations we have the temperature at the center of the plate to be 51 ^{0}C and from the simulations it is very close to 52^{0}C

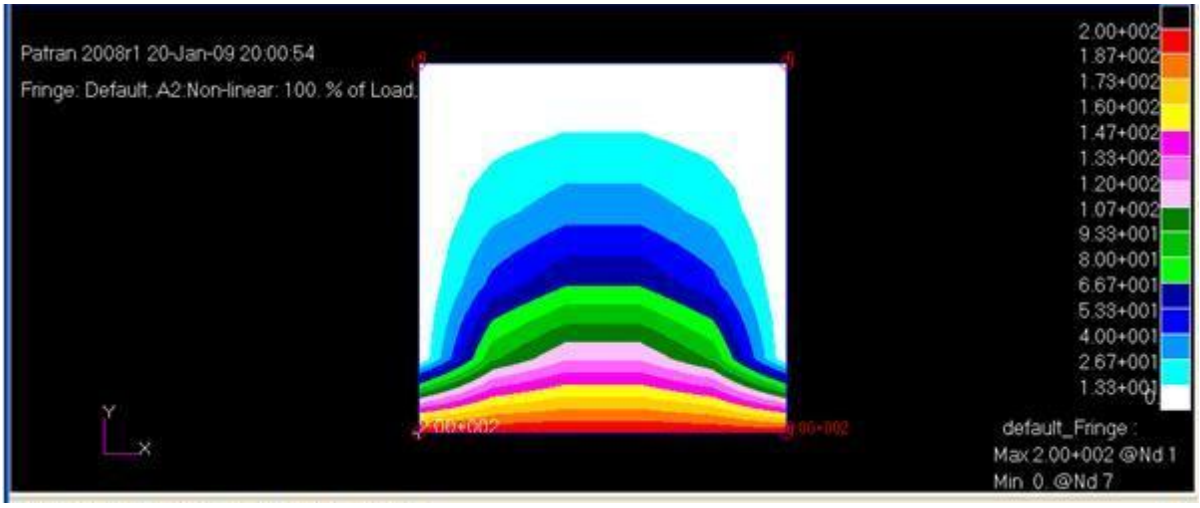

Radiation:

To validate the radiation model we again consider a plate. A heat flux is applied on the plate which is equivalent to a radiation at 293 K. A very high value of conductivity is given to the plate. In steady state, ideally the temperature of the plate should be 293 K. From the simulations we get the same result.

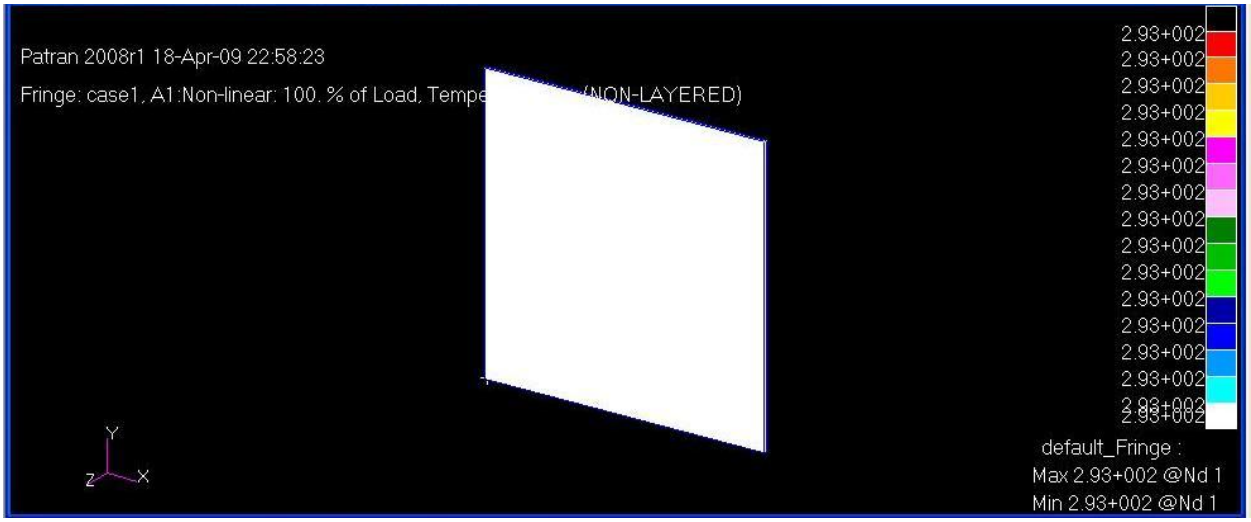

3.1.10 Grid Convergence

A grid convergence study was carried out. Grid convergence essentially means that even if go on making the grid finer and finer the solution does not change. Initially we had a grid of 352

elements and maximum size of an element being 6 cm. We carried out the same simulations on a grid of 478 elements and maximum size of elements was 4 cm. The results were exactly the same and hence the 6 cm grid results do not have errors in them because of the grid.

3.2 Design

So far we have looked at the obtaining the temperature of the body of the satellite. The next step is to model the whole body of the satellite. From our past experience, we understand that modeling such a complicated geometry would be difficult. If it is not possible to do so, here is an alternate methodology to model the complete satellite. Each PCB will be evaluated in a fashion similar to that of the battery box (discussed in Chapter 4). After that we can obtain the heat flux from that PCB to the satellite. The updated satellite temperature will be calculated using this additional heat flux and the temperature of the PCB will be calculated again. This will go on until convergence. That is the heat fluxes to the satellite from two consecutive iterations are very close to each other. This will be done for all the PCB's. The heat dissipation terms will be taken care during the modeling of the individual PCB's.

Thus after eliminating all the assumptions we would obtain the temperatures of the body of the satellite. The temperature is expected to be higher as compared to model1 since extra heat dissipation terms and additional fluxes have to be accounted for. The temperature obtained would be higher than we would have liked. So an optimal amount of OSR would be applied so as to bring the temperature down to the desirable limits. The effects of coating the satellite with OSR have already been studied.

3.3 Conclusion

It is really difficult to make sense out of simulation results and validating them. A lot rests on this simulation as they are the first step in determining what thermal control measures need to be taken. Thus it is absolutely essential to get the results of these simulations as accurately as we can. Efforts have also been made to write our own code. The issue with the code is that we haven't been able to validate it yet. In the next chapter we will look in the thermal control design of one of the critical components from the thermals perspective, the battery box.

4. Battery Box Design

In this chapter, we shall discuss the thermal control design of the battery box. In order to design thermal control, we first need to obtain the temperatures of the battery box. Two approaches are used to obtain the same. The first one is a theoretical approach where the exact solution of the differential equation is obtained. It is not possible to solve the differential equation if we incorporate the heater in the model. The second approach is by a MATLAB code. The results from the first approach will be used for validating the code. In a later section, the feasibility of the design shall be discussed.

4.1 The model

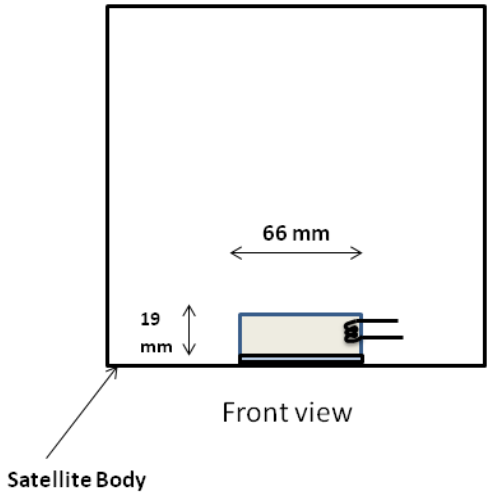

Figure 5: Front view of battery box

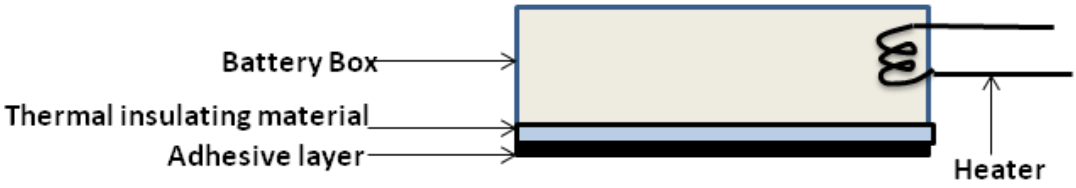

Figure 6: Battery Box layout

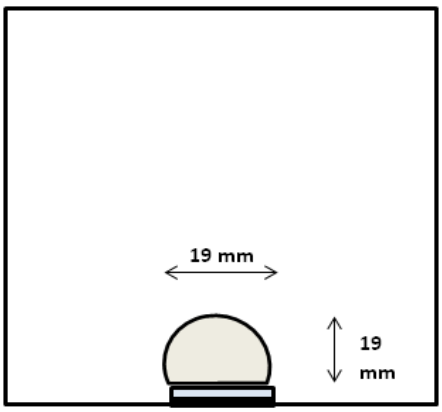

Figure 7: Side view of battery box

The battery box of the satellite is comprised of four batteries and an outer cover. The dimensions of the battery box are as shown in the figure. The material used for the outer cover is Aluminum.

4.2 Assumptions

In this analysis, the spatial gradients in the battery box have been neglected. The radiation terms have also been dropped to simplify the analysis. The temperature of the body of the satellite is assumed to be sinusoidal. The maximum and the minimum temperature of the satellite body are assumed to be 312 K and 272 K respectively. This analysis is applicable once the satellite is out of detumbling mode.

4.3 Nomenclature

- Tsat – Temperature of the satellite (K)
- Tbat – Temperature of the battery box (K)
- M – Mass of the battery box including the mass of the batteries = 0.6 kg
- C – Specific heat capacity = 898 J/(kg-K)
- P – Power provided by the heater (W/m^2)
- h – Internal heat dissipation of the batteries = 0.01 W on an average
- R – Effective thermal resistance (Insulation + Adhesive) (K/W)
- K = 1/R
- Omega – angular velocity of satellite = 0.000978 rad/sec
- t – Time

- Average – Average temperature of the body of the satellite
- Amplitude – Amplitude of the sinusoid

4.4 Governing equation

$$MC\frac{dTbat}{dt} = h - K(Tbat - Tsat)$$

And from the assumptions we have

$$Tsat = 292 + 20\sin(Omega * t)$$

4.5 Theoretical Calculations

The solution of this initial value problem is given by

$$Tbat = (hR + Average) + \frac{Amplitude\,(\sin(Omega * t) - c * \cos(Omega * t))}{1 + c * c} + d(t)$$

where,

$$c = MCR * Omega$$

and d(t) represents the exponentially decaying transient. The constant of integration is incorporated in d(t).

The results of the theoretical calculations will be presented along with the results of the MATLAB code (Refer to Appendix B for the code)

In the code, the time derivative of the governing equation has been approximated using the forward difference method. The initial temperature of the battery box is assumed to be 300 K.

4.6.1 Validation using Theoretical calculations

For validation purposes, the value of P was set to zero and the two plots were compared.

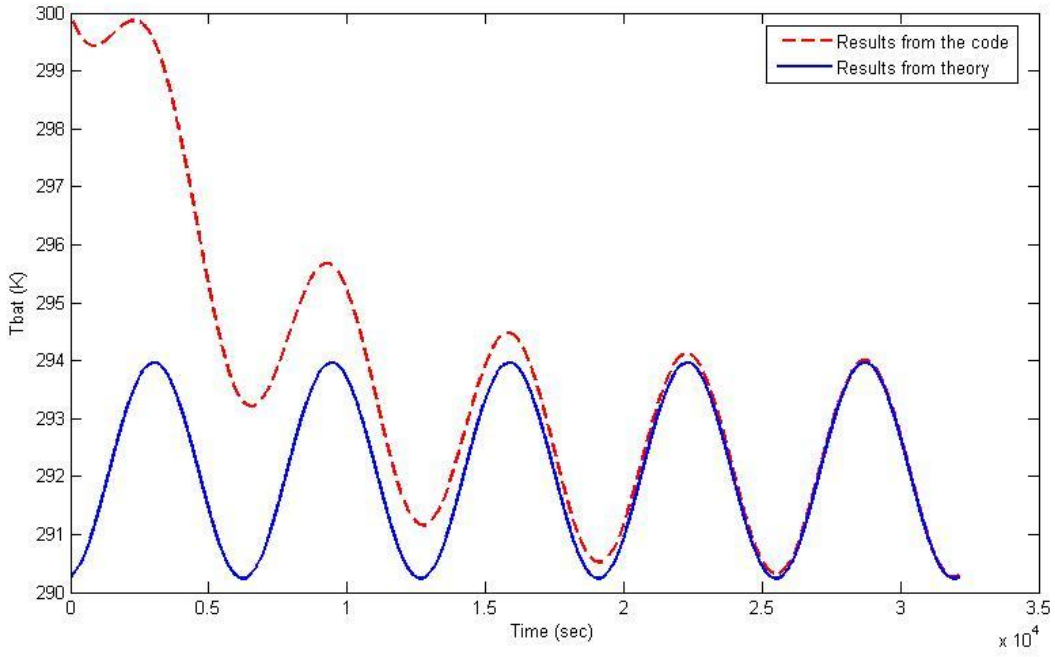

The theoretical results have been computed here while neglecting the transient terms. Thus we can see that the results obtained from the code exactly match the results from theory in the steady state. If the transient terms were included while computing Tbat from theory, the results would have matched in the transient region as well.

4.6.2 Parametric study

The effects of varying K (effective conductance) and P (input power of the heater) have been studied.

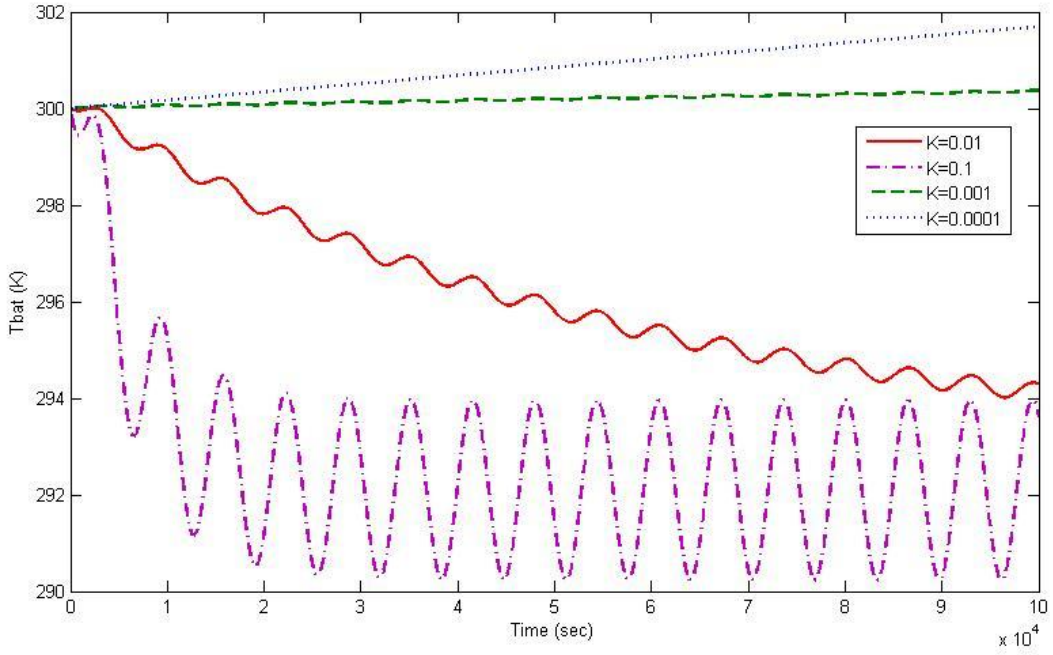

As we can see from the above diagram, the conductivity of the insulation will play a critical role. If the value of K is relatively high, then the range of temperature goes on increasing, after a particular value of K, the heater will become a necessity. As we go on decreasing K, the time required to attain steady state will go on increasing but the difference between the maximum and minimum temperature will go on decreasing. Thus in this case a lot will be governed by the initial temperature of the battery box. As we decrease it even further, the system becomes unstable. This is because the conduction term becomes insignificant and the system dynamics is governed by the heat generation terms. For these temperatures the optimum value of K is 0.1

A similar study was carried out for P as well. For this case heater was not required at all. But we still plan to have a heater just for safety. An optimum P can be calculated if the temperature cannot be maintained within bounds by the insulation alone. The typical value of average power required is of the order of milliwatts even when the satellite temperature varies from 240K to 360 K. Thus even if a heater is required, the power consumption by the heater will not be critical

4.7 Conclusion

It is very clear from the results that a heater may not be required if an appropriate insulation is chosen. But as a factor of safety we plan to have a heater for the battery box. Even if we have a

heater, the power requirements of the heater are very small. In the next chapter we shall look into the different thermal coatings available and also a heater circuit which meets our requirements.

5. Thermal coatings and Heaters

5.1 Paints and coatings

The conduction model of the battery box assumes the radiation terms in heat exchanges to be very small. In order to ensure that minimum heat exchange takes place through radiation, thermal control paint of appropriate emittance and absorbance value will be applied to the surfaces of the battery box.

Inorganic white AZ-93 coat manufactured by AZ Technologies seems suitable for application on outer surface of battery box. Electrically conductive paints are not required for battery box as the battery box is within the satellite.

5.1.1 AZ -93

AZ-93 is an inorganic white thermal control paint developed for use on spacecraft surfaces exposed to the deleterious effects of the space environment. Application of AZ-93 creates a nonspecular white coating that provides superior thermal protection by allowing only 14-16% of the solar radiation impinging on the spacecraft external surface to be absorbed through to the interior systems while emitting 89-93% of the internal heat generated to the cold vacuum of space. By incorporating a highly stabilized pigment system with a silicate binder, AZ-93 forms a bendable ceramic coating that has been tested time and again and has proven itself stable in the harshness of the space environment. AZ-93 has been exposed by NASA to atomic oxygen (AO) fluence of 5.6 x 1022 atoms/cm2, charged particle radiation of 4.5 x 1015 e-/cm2, and vacuum ultraviolet (VUV) radiation (from 118 nm to 170 nm) of 701 equivalent solar hours with less than 4% deterioration in solar absorptance (αs) and less than 1% change in thermal emittance (εt).

Nominal Surface Resistivity ~1013 _/sq
Thermal Emittance - 0.91 ± 0.02
Solar Absorbance - 0.15 ± 0.02 at _ 5.0 mils thickness
Use Temperature Range -180 C to 1400 C
Appearance/Color Nonspecular white
Nominal Dry Thickness 5.0 ± 1.5 mils (over 85% of coated area)

ASTM D3359A Adhesion Grade Not less than 3A

Full Cure 7 days

5.2 Heater for the battery box

The conduction model results show that a heater is not needed for the battery box. However it is being included as a safety measure.

5.2.1 Heater

Polyimide thermofoil heater has been selected for use for the battery box. Polyimide (Kapton) is a thin, semitransparent material with excellent dielectric strength. Polyimide Thermofoil™ heaters are ideal for applications with space and weight limitations, or where the heater will be exposed to vacuum, oil, or chemicals.

5.2.2 Polyimide thermofoil heater

- Thin, lightweight heaters allow you to apply heat where it's needed, reducing operating costs
- Etched-foil heating technology provides fast and efficient thermal transfer
- Custom profiling gives uniform thermal performance of the heating output to improve processing yields and productivity
- FEP internal adhesive for use to 200°C (392°F)
- Radiation resistant to 10^6 rads if built with polyimide insulated leadwire
- Very small sizes available

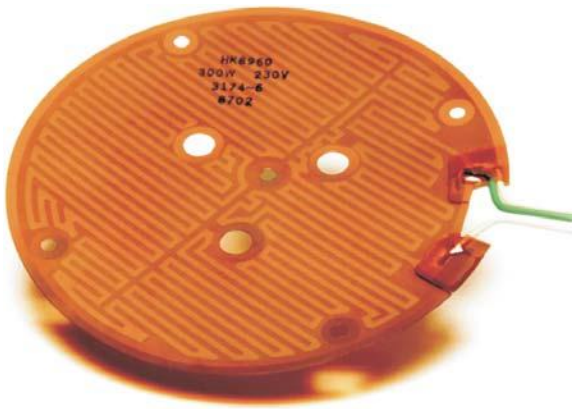

Figure 8: Kapton Heater

5.2.3 Thermal sensor

The heater solution proposed uses RTD as the sensor.

Resistance temperature detectors (RTDs)

An RTD sensing element consists of a wire coil or deposited film of pure metal. The element's resistance increases with temperature in a known and repeatable manner. RTDs exhibit excellent accuracy over a wide temperature range and represent the fastest growing segment among industrial temperature sensors.

RTD element types

Platinum is the most widely specified RTD element type due to its wide temperature range, stability, and standardization between manufacturers. Copper, nickel, and nickel-iron can offer comparable accuracy at lower cost in many applications.

Platinum RTD sensor		Thermistor sensor	
2°C	0.02 V	25°C	0.25 V
50°C	0.50 V	50°C	0.50 V
100°C	1.00 V	75°C	0.75 V
200°C	2.00 V		
Accuracy:	±1% of span	Accuracy:	±2% of span
Linearity:	±0.1% of span	Linearity:	±2% of span

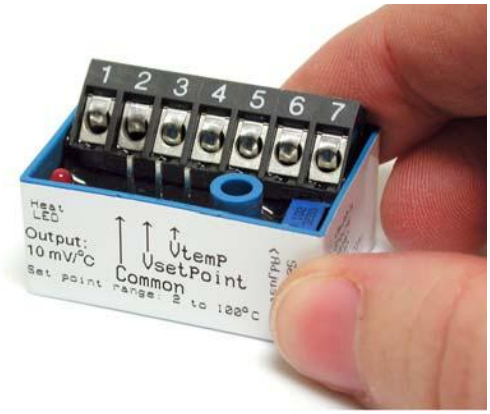

Figure 9: Thermal control unit

5.2.4 Thermal control unit

The CT325 Miniature DC Temperature Controller of Minco Technologies has been selected for controlling the battery heater. The CT325 Miniature DC Temperature Controller is designed for use with Minco Thermofoil™ heaters and RTD or thermistor sensors. It offers inexpensive on/off temperature control of your process or equipment with accuracy many times better than bimetal thermostats. The entire unit is epoxy filled for moisture resistance, with a through-hole for a mounting bolt. A terminal block provides the power input, sensor input and heater output

connections. We easily read and adjust the set point temperature using a voltmeter, and then monitor the actual signal temperature at the other end. Operating from a 4.75 to 60 volt DC power supply, the controller can switch up to 4 amps power to the heater.

6. Study of possible failures

Even after detailed simulations, there may be many possible modes of failures which need to be tested for. Here the failure is in not meeting the requirements to be met by the thermals subsystem. It may not necessarily lead to failure of the satellite as a whole. Failures can be broadly classified into four categories:

- Improper maintenance of temperatures throughout the lifetime of the satellite
- Failure due to thermal stresses
- Errors in thermal analysis
- Failure of thermals hardware like coatings, paints and heater

6.1 Improper maintenance of temperatures throughout the lifetime of the satellite

These failures may arise due to improper use of thermal coatings and paints. The choice of coatings and paints come from the analysis on simulations. The simulations may be not an exact representative of reality. Failures in this category can be further sub-categorized as:

- Failure of the heater to provide adequate heat to the battery at proper times due to an error in the temperature sensor
- Accumulation of heat due to faulty conduction and radiation mechanisms
- Thermal losses due to wiring

6.2 Failure due to thermal stresses

It is not possible to comment much on the reasons for this failure as thermal stress analysis is still pending. The possible modes are:

- Local buckling due to thermal stresses
- Fatigue due to cyclic thermal loading

6.3 Errors in thermal analysis

Thermal analysis has been carried out for predicting the temperature of the satellite using MSC NASTRAN. A lot of simplifications and assumptions have been made in the process. A few examples include not accounting for the Albedo (the solar flux that is reflected from the surface

of the earth onto the satellite), or the effects of radiation not considered while modeling the battery box. These need to be accounted for before finally choosing the coating required to maintain optimum temperature. This is the root cause for the other modes of failure as well. The causes of this mode of failure are:

- Improper boundary conditions applied for analysis
- Modeling errors
- Errors in interpretation of results

6.4 Failure of thermal hardware

Failure due to thermal hardware is failure due the thermal coatings, paints, sensor and heater used. These can be subdivided into:

- Degradation of materials over time
- Improper characterization of thermal properties
- Error in method attachment
- Contamination of coatings and paints on or before launch

6.5 Conclusion

All the modes of failure expect that of thermal hardware can in some way be attributed to the error in analysis. The mistake in prediction of the temperature of the body of the satellite which is the first step of the design process is bound to propagate further. Improper thermal analysis implies incorrect choice of coatings which can lead to failure due to very high or very low temperatures. These very high or very low temperatures can lead to very high thermal stresses and the satellite may fail due to local buckling or fatigue. Thus it is very essential to accurately determine the temperature of the body of the satellite.

The next important mode of failure is that due to thermal hardware. Characterization of material properties is essential. As shown in the analysis of the battery heater, a change in the property of the coating used can lead to very high or very low temperratures. Thus after determining the properties of coating required from the simulations, it is necessary to obtain a material with those properties within acceptable limits. The method of attachment may be improper which may lead to bad conduction paths.

The other two modes of failure stem from the failure in analysis. Fatigue is highly improbable unless the thermal stresses are very high. Typical materials are able to withstand around 10e6 cycles. The design period of the satellite is 4 months which translates to around 1600 cycles. Thermal sensors are generally very accurate. The probability of the failure of the thermal sensor is very low.

From this it is evident that a lot of effort has to be put into thermal analysis and validation of the analysis. It is also necessary that the thermal analysis be backed by testing as well for validation purposes. This shows the importance of testing methods. In the next chapter we shall discuss the thermal tests that must be carried out for the qualification model.

7. Thermal Testing

The previous chapter has reiterated the importance of thermal testing. It is imperative to back the analysis with proper testing. Testing can also be thought of as a validation of the analyses done. It is mandatory for the qualification model to undergo certain tests. There are three types of tests which can be carried out on the satellite

- Thermovacuum test
- Solar Simulation test
- Heat transfer measurement test

These tests have been listed in their relative order of importance with the Thermovacuum test being the most important.

7.1 Themovacuum Test

An economical and straightforward testing technique must be employed to perform the qualification and acceptance thermal vacuum tests on protoflight model of a micro-satellite. In space, far from the earth's surface , the pressure is around 10^{-13} mbar and the temperature about 4^{o} K, only taking the radiation temperature into account since space is virtually opaque in the optical sense. The simulation of such complex and environmentally variable conditions is technologically non-viable, therfore a thermal vacuum chamber is required to simulate the environmental conditions faced by the satellite during its orbit.

7.1.1 Thermal Vacuum Chamber

This testing facility has an aluminum-made thermal shroud, internally black painted to a higher value of emissivity, which is able to cycle and to be controlled from liquid nitrogen temperature to +150 C under a vacuum conditioning in the 10−6 mbar range or better. The testing of this facility in terms of producing thermal soaks at intermediate temperature levels is very useful for this particular application, once the thermal gradients between the T/V chamber shroud and the satellite could minimized

7.1.2 Thermal Radiant Heat Plates

Radiative heat panels powered by surface attached skin-heaters are very reliable heating devices. With the skin-heaters providing an average thermal dissipation up to 5W/in2, the radiative

panels, painted to a black surface with high values of emissivity, are able to produce consistent radiant heat fluxes under very good control. In order to produce the required heat input to the spacecraft as a simulation of the environmental radiation to its external surfaces (case of TBT) or just to participate on the temperature adjustment for the thermal conditioning of the subsystems (case of TCT), a set of four individual heating panels is built in this way facing the lateral sides of the spacecraft . Each one of the four individual panels has four (two upper and two lower) Kapton_-based skin-heater films attached to its internal surface. As a result, this rectangular shaped test rig has an upper zone made by a set of eight skinheaters and a lower zone also made by a set of eight skin-heaters. For each zone, the skin-heaters are electrically interconnected and powered by a DC power supply.

In order to improve the radiant heat transfer between the panels and the T/V chamber thermal shroud, condition required to speed-up the transitions between the distinct test phases, the outside faces of the radiant panels are black painted to a high value of thermal emissivity

7.1.3 Electrical Ground Support Equipment

During the execution of the Themocycling tests of the satellite, pre-defined electronic functioning tests should be performed on its subsystems. These are accomplished through the use of the EGSE .This dedicated test station is physically installed next to the TVC and then connected to the spacecraft under test by using cables and the chamber feedthroughs

7.1.4 Test Instrumentation

In order to get the necessary data from the test, various thermocouples type T were installed on the subsystems, radiant heat plates and other test setup locations, plus another 16 thermocouples installed on the T/V chamber shroud to control and monitor its thermal conditioning. For the thermal control of the radiant heat plates, some thermocouples are taken to two temperature controllers, in a number of eight thermocouples for the upper zone and eight for the lower zone. Functioning test cables are properly run and connected from the subsystem to the EGSE (Electrical Ground Support Equipment).A data scanner is used to collect and to send data to a PC-based computer for processing, displaying in real time, and storage for further recall. For this particular test, all 124 channels were scanned every 30 s.

Besides the standard data acquisition system (DAS), a simple but reliable 20-channel digital temperature recorder is installed, to which additional temperature sensors coming from selected and critical parts of the spacecraft and the test setup are connected for redundancy. This additional data acquisition system, connected to a separated power supply, is programmed to print data every 15 min, or every 30 s in case of facing an emergency situation

7.2 Solar Simulation Test

Solar simulation test is performed to verify the spacecraft thermal design and the thermal mathematical model which will be used to predict the "on orbit" temperatures. The extreme condition has been simulated by applying a certain quantity of kapton tape on the north radiator in order to increase its solar absorptance up to the extreme values. Different seasonal conditions (i.e. solar fluxes cases) and transient conditions have been properly simulated throughout the test in order to verify the spacecraft thermal control performances.

A Large Space Simulation Chamber (LSSC) with 4-meter solar beam expandable to 4.5 meters is being present at ISRO Satellite Center, Bangalore. The solar simulator consists of lamp modules, transfer optics and douser, all housed in a protected environment inside the lamphouse, and the main chamber window located in the spout along with the collimating mirror located inside the auxiliary chamber. There are eleven 20-KW Xenon lamp modules for use with 4-meter beam size, which may be increased to fourteen 20-KW Xenon lamps to expand the beam to 4.5meters. In either configuration the intensity range of 0.65 KW/M 2 to 1.7 KW/M 2 is provided with intensity uniformity of ± 4% in the reference plane at the center of the main chamber. The collimating mirror is fabricated as a mosaic of 55 hexagonal mirrors positioned onto the mirror support structure supported inside the auxiliary chamber on a kinematic mount. The mirrors are made of an aluminum alloy, diamond turned and subsequently aluminized and anti-reflection overcoated for protection. The mirrors and the support structure are held at ambient temperature except during the mirror degas mode. Lamp modules, transfer optics and lamp house panels are cooled by closed loop D.I. Water System exchanging heat with the facilities refrigerated water supply.

7.3 Heat transfer Measurement Tests

This test is performed to determine the various heat transfer aspects involved in the thermal design of the satellite, which would be used in the determination of thermal resistance and conductivity along with its variation with temperature. Steady state guarded heat flow meter method is used for the test.

A sample of the material to be tested is held under a reproducible compressive load between two polished metal surfaces, each controlled at a different temperature. The lower contact surface is part of a calibrated heat flux transducer. As heat flows from the upper surface through the sample to the lower surface, an axial temperature difference across the sample along with the output from the heat flux transducer, thermal conductivity of the sample can be determined when the thickness is known."Measurement is done at cryogenic & elevated temperatures
in high vacuum or in inert gas or in atmospheric environments

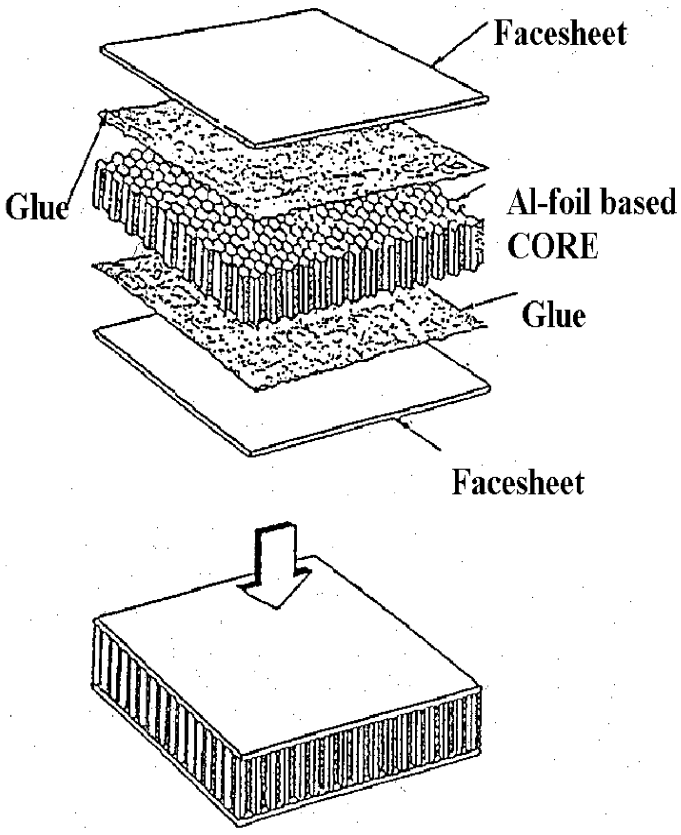

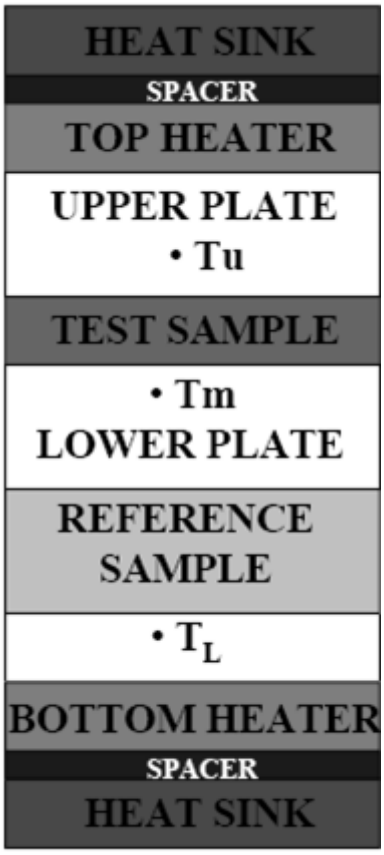

Using the heat flux equations, the thermal resistance of various materials can be obtained at different temperatures. This test facility is also available at ISAC, Bangalore.

8. Conclusion

A lot is dependent on the results obtained from simulations. Thus simulations will play a key role in deciding the success of the thermals sub-system. It is absolutely essential to incorporate internal radiation in the simulation models. The problem here is that we are unable to understand the reason for the model not working. The battery box design has been studied in detail and the simulations show favorable results. Possible modes of failure have been identified and it is anticipated that the chances of failure due to simulations is very high. For all these reasons, there has to be a concrete validation for the simulations, and testing is the way out. Testing methods have also been studied in detail. The work ahead is to obtain detailed thermal simulation, come up with the optimal thermal design in order to maintain the temperature of the satellite within desirable limits to satisfy the requirements imposed by the other sub-systems on the thermal sub-system. In the end I would like to quote Mr James Cantrell (Main engineer, US-Russian joint mission) “Most of major spacecraft failures are not due to technological surprises but due to simple and usually manual engineering faults often neglected for their simplicity”.

9. Appendix

9.1 Appendix A – Calculation of solar flux

The orbit:

The satellite is assumed to be placed in a 10.30 am, 98° polar Sun synchronous orbit at an altitude of 670 km.

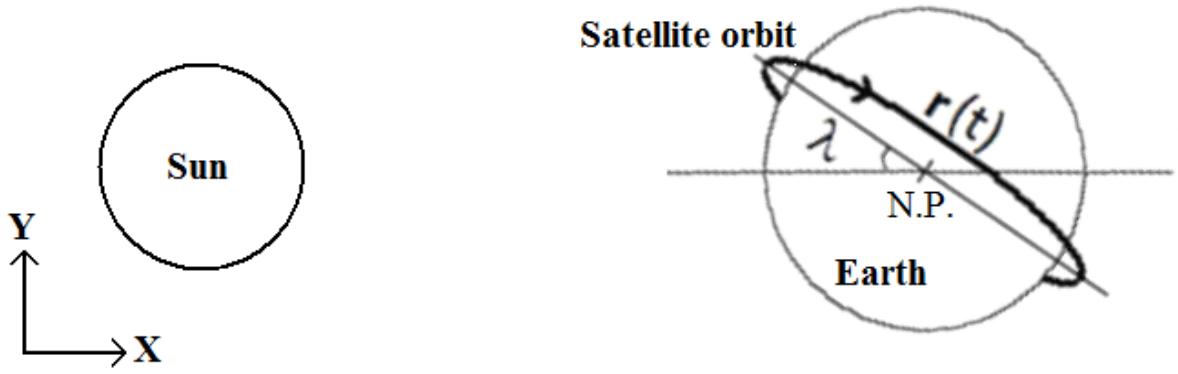

Figure 10: Satellite orbit

An Earth-centred coordinate reference is chosen with the XY plane as the plane of Earth's orbit. The line joining the Sun's and the Earth's centres is fixed as the X axis. For a Sun-synchronous orbit, the angle λ is a constant and equals 22.5° for the 10.30 am orbit.

The position of the satellite as a function of time is given by:

$$\therefore \vec{r}(t) = R\begin{bmatrix} \cos\lambda & \sin\lambda & 0 \\ -\sin\lambda & \cos\lambda & 0 \\ 0 & 0 & 1 \end{bmatrix}\begin{bmatrix} \sin(\omega t) \\ \cos(\omega t)\sin 8^\circ \\ \cos(\omega t)\cos 8^\circ \end{bmatrix} = R\begin{bmatrix} \cos\lambda\sin(\omega t) + \sin\lambda\cos(\omega t)\sin 8^\circ \\ -\sin\lambda\sin(\omega t) + \cos\lambda\cos(\omega t)\sin 8^\circ \\ \cos(\omega t)\cos 8^\circ \end{bmatrix} \quad \ldots(1)$$

Here, R = 6400km + 670km = 7070km. The time t = 0 is when the satellite is closest to the North Pole (N.P.) and ω is the angular speed of the satellite.

The effect of direct solar radiation is calculated first. And then the correction due to the light reflected by the Earth is added.

Direct solar power incident at any point of time:

It can be easily seen that, if the nadir surface always faces the Earth, the power at any point in space $\vec{r} = (x, y, z) = R(\cos\alpha, \cos\beta, \cos\gamma)$ depends only on two angles: the angle of the **r** with the direction of the sun-rays which is α and another local angle (i.e. an angle related to the orientation of the satellite in space and not its position) denoted as φ. Hence, to find the power at (x, y, z),we can simply find the power at the more convenient position $\vec{r}' = \left(x, \sqrt{y^2 + z^2}, 0\right)$.

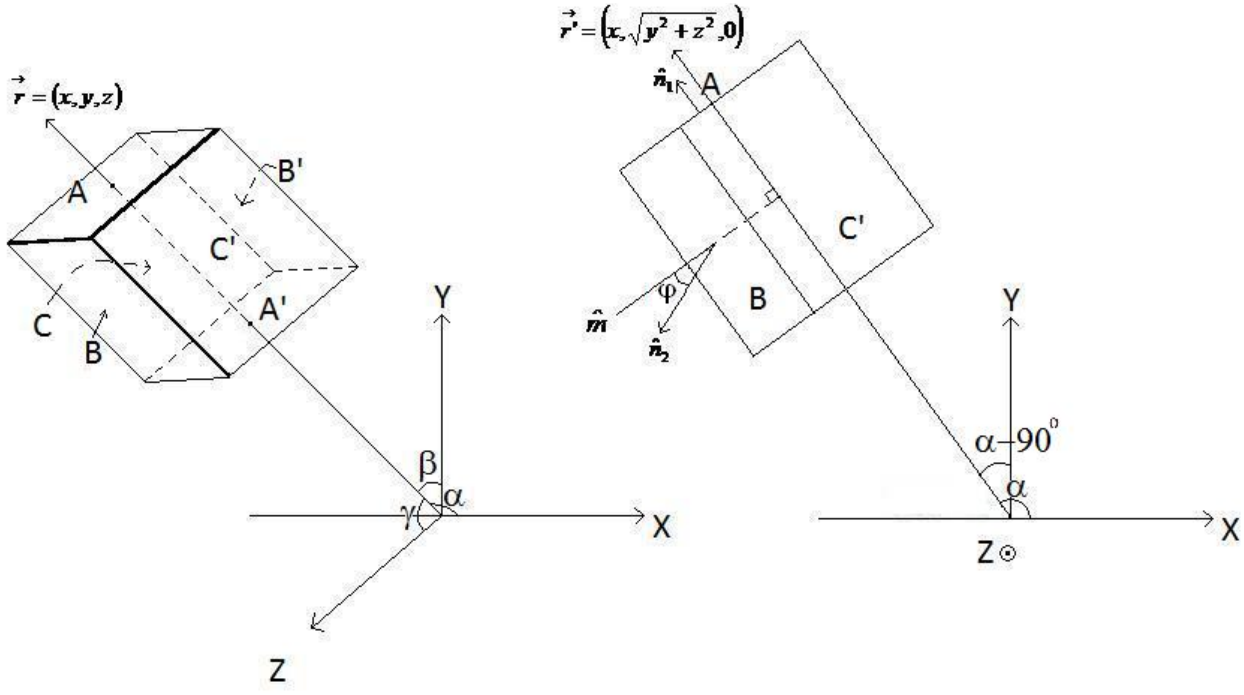

Figure 11: Normal vectors for different faces for flux computation

Let $\hat{n}_1, \hat{n}_2, \hat{n}_3$ be the normal vectors of the Sun-facing faces A, B and C of the satellite. $\hat{m}$ is the unit vector in the XY plane and perpendicular to $\hat{n}_1$.Thus, if the satellite rotates about the axis defined by its position vector $\vec{r}'$ by an angle φ, the angle between $\hat{n}_2$ and $\hat{m}$ changes by φ. The normal vectors are found to be:

$$\hat{n}_1 = (\cos\alpha, \sin\alpha, 0)$$
$$\hat{n}_2 = (-\sin\alpha\cos\varphi, \cos\alpha\cos\varphi, -\sin\varphi)$$
$$\hat{n}_3 = (-\sin\alpha\sin\varphi, \cos\alpha\sin\varphi, -\cos\varphi) \quad \ldots(2)$$

At any time, out of each pair of opposite faces, only one face receives sunlight. Thus, for the three pairs of faces, the intensity of sunlight on the sunlit face is

$$I_1 = -S\cos\alpha$$
$$I_2 = S|\sin\alpha\cos\varphi|$$
$$I_3 = S|\sin\alpha\sin\varphi| \quad \ldots(3)$$

where S = 1353 W/m^2

From (1),

$$\cos\alpha = \cos\lambda\sin\omega t + \sin\lambda\cos\omega t\sin 8°$$
$$= 0.924\sin\omega t + 0.053\cos\omega t$$
$$= 0.925\sin(\omega t + 3.3°)$$

Thus from this and (3), we can find $I_1(t)$, $I_2(t)$ and $I_3(t)$. Here, φ is a variable and the satellite can rotated such that maximum amount of sunlight is incident on the solar panels. This condition is satisfied at φ = 45°. For this condition,

$$I_1 = -S\cos\alpha$$
$$I_2 = S\frac{\sin\alpha}{\sqrt{2}}$$
$$I_3 = S\frac{\sin\alpha}{\sqrt{2}}$$

On the other hand, the worst case power is incident when φ = 0° or φ = 90°. For these conditions,

$$I_1 = -S\cos\alpha \qquad \text{or} \qquad I_1 = -S\cos\alpha$$
$$I_2 = S\sin\alpha \qquad\qquad I_2 = 0$$
$$I_3 = 0 \qquad\qquad I_3 = S\sin\alpha$$

The time for which the satellite is eclipsed is now calculated.

Calculation of the eclipsed region:

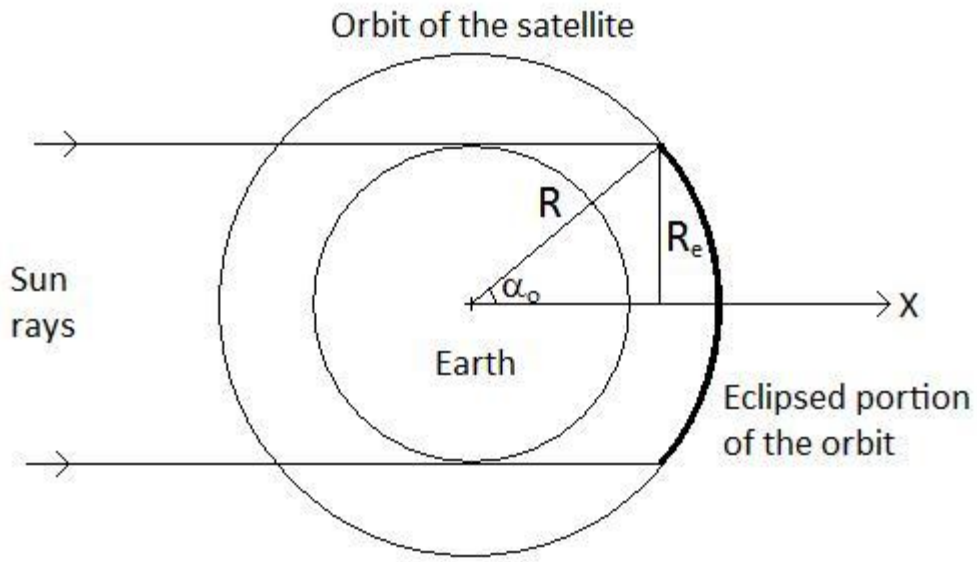

Figure 12: Eclipsed region of the satellite

$$\alpha_0 = \sin^{-1}\left(\frac{R_e}{R}\right) = \sin^{-1}\left(\frac{6400}{6400+670}\right) = 64.8°$$

Hence, the satellite is in eclipsed region when

$$\alpha < \alpha_0$$
$$\Rightarrow \cos\alpha > \cos\alpha_0$$
$$\Rightarrow 0.925\sin(\omega t + 3.3°) > 0.425$$
$$\Rightarrow \sin(\omega t + 6°) > 0.46$$
$$\Rightarrow 27.39° < \omega t + 3.3° < 152.61°$$
$$\Rightarrow 24.09° < \omega t < 149.31°$$

Using this, the intensity of direct sunlight incident on the faces is found.

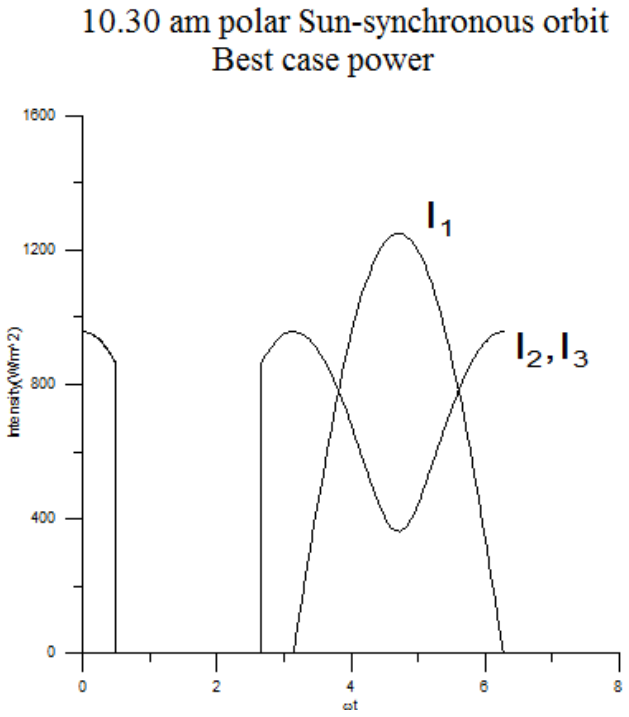

Figure 13: Solar flux incident on the satellite

9.2 Appendix B- MATLAB code for heater

```
Average= 292;

Amplitude= 10;

omega=6.28/(107*60);

for i=1:32118

   Tsat(i)=Average+Amplitude*sin(omega*i);

end

h=0.01;

K=0.1;

P=2;

M=0.6;

C=898;

c=M*C*omega/K;

for j=1:32118

   Tbat(j)=300;

   Power(j)=0;

end


for ii=2:32118

    if(Tbat(ii-1)<288)

        Tbat(ii)=Tbat(ii-1)+((P+h)/(M*C)-K*(Tbat(ii-1)-Tsat(ii-1))/(M*C));

        Power(ii)=1;
```

```
    else
        Tbat(ii)=Tbat(ii-1)+(h/(M*C)-K*(Tbat(ii-1)-Tsat(ii-1))/(M*C));
        Power(ii)=0;
    end
    Tbattheo(ii)=(h/K+Average)+Amplitude*(sin(omega*ii)-c*cos(omega*ii))/(1+c*c);
end
Tbattheo(1)=Tbattheo(2);
plot(Tbat)
hold on
plot(Tbattheo)
```